Strain distributions in the InAlN barrier layers of In$_{0.17}$Al$_{0.83}$N/GaN heterostructure field-effect transistors

Yang Zhou[1,2] · Zhe Xu[1,2] · Juntao Li[1,2]

Abstract

Using measured gate-source capacitance–voltage (C–V) curves and forward current–voltage (I–V) curves for In$_{0.17}$Al$_{0.83}$N/GaN heterostructure field-effect transistors (HFETs) of various gate lengths with normal-Ohmic contacts and side-Ohmic contacts, the strain distributions in the InAlN barrier layers are analyzed. It is found that the compressive strain in the InAlN barrier layer is nearly uniformly distributed between source and drain contacts for devices with side-Ohmic contact processing while it is enhanced and monotonously decreased from the middle to the source/drain contact for devices with normal-Ohmic contact processing. This difference in the strain distributions is attributed to the difference in the lateral diffusing of Ohmic contact metal atoms into the InAlN barrier layer during the different Ohmic contact processing.

1 Introduction

AlGaN/GaN heterostructure field-effect transistors (HFETs) have made tremendous progress and been adopted in high frequency and high power applications over the past few decades. However, due to the piezoelectric and converse piezoelectric nature of the GaN material [1–3], strain-related structural changes of the AlGaN layer are detrimental to the device performance and reliability [4–7]. InAlN with a composition of 17% Indium grown on GaN is supposed to be free of strain [8, 9] and InAlN/GaN HFETs can offer more promising reliability benefits over the conventional highly strained AlGaN/GaN HFETs. The median time to failure for InAlN/GaN HFETs was reported to be 8.9×10^6 h at junction temperature of 150 °C [10]. We have previously found that a compressive strain exists in the InAlN barrier layer of the In$_{0.17}$Al$_{0.83}$N/GaN HFET [11]. As a result, strain-induced problems are inevitable for InAlN/GaN HFETs as well. Little attention, however, was given to the strain properties of InAlN/GaN HFETs. Therefore, it is highly essential to get further understanding of the strain information in InAlN/GaN HFETs as much as possible.

In this study, the strains in the InAlN barrier layers of In$_{0.17}$Al$_{0.83}$N/GaN HFETs with different gate lengths are determined and compared between devices with normal-Ohmic contacts and with side-Ohmic contacts. The method used here to evaluate the strain was first proposed in the analysis of interface trap states in InAlN/GaN heterostructures [11] and subsequently adopted to investigate the strains in the AlGaN barrier layers of AlGaN/GaN HFETs [12]. It is found that the compressive strain in the InAlN barrier layer is nearly uniformly distributed between source and drain contacts for devices with side-Ohmic contact processing while it is enhanced and monotonously decreased from the middle to the source/drain contacts for devices with normal-Ohmic contact processing.

2 Experiments

The InAlN/GaN epi-structure used in this work was grown on a sapphire substrate by MOCVD. Detailed structural information is shown in Fig. 1. A two-dimensional electron gas (2DEG) density of 1.02×10^{13} cm^{-2} and an electron mobility of 1900 cm^{2}V^{-1} s^{-1} were obtained by Hall measurements. InAlN/GaN HFETs with normal-Ohmic contacts and side-Ohmic contacts [13] were prepared. In the device with side-Ohmic contacts, as shown in Fig. 1, Ohmic metals directly touch the 2DEG channel. The detailed device fabrication processing is the same as described in [14]. The side-Ohmic contact processing employed a 150 °C lower

✉ Yang Zhou
    zhouyang@mtrc.ac.cn

1   Microsystem and Terahertz Research Center, China
    Academy of Engineering Physics, Chengdu 610200, China

2   Institute of Electronic Engineering, China Academy
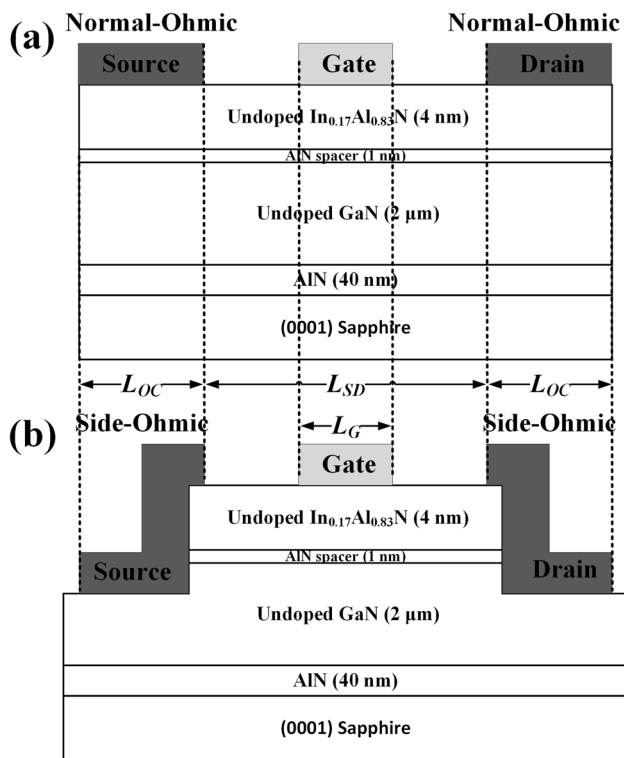   of Engineering Physics, Mianyang 621900, China

Fig. 1 Cross sections of prepared InAlN/GaN HFETs with normal-Ohmic contacts (**a**) and with side-Ohmic contacts (**b**)

rapid thermal annealing temperature than the normal-Ohmic contact processing and achieved a specific resistivity of the same level($\sim 5 \times 10^{-5}$ $\Omega \cdot$cm^2). Devices with different types of Ohmic contact processing are both rectangular with the same sizes. The source and drain Ohmic contacts with the dimension of 50 μm long (L_{OC}) and 100 μm wide (W) are 100 μm (L_{SD}) apart. The gate Schottky contact is located in the middle between the source and drain. Devices with different gate lengths (L_G) of 20 μm, 40 μm, 60 μm and 80 μm are, respectively, labeled as sample A1, A2, A3 and A4 for normal-Ohmic contacts and sample B1, B2, B3 and B4 for side-Ohmic contacts. Capacitance–voltage (*C–V*) and current–voltage (*I–V*) measurements are performed using Agilent B1520A at 1 MHz frequency and B1500A, respectively.

3 Results and discussions

Using the *C–V* measurement and the forward *I–V* measurement for the gate-source diode and the polarization theory of GaN-based heterostructures [1, 2], the piezoelectric polarization of InAlN barrier layer in the InAlN/GaN HFET can be determined and consequently the in-plane strain of the InAlN barrier layer can be evaluated [15]. The method to determine the in-plane strain of the

InAlN barrier layer is described as below. The polarization sheet charge density σ/e at the interface between InAlN and GaN at zero bias can be calculated using the following equation [16]

$$\sigma/e = n_{2DEG} + \left(\frac{\varepsilon_s \varepsilon_0}{de^2} \right) (e\phi_b + E_F - \Delta E_c) \quad (1)$$

where

n_{2DEG} is the two dimensional-electron gas (2DEG) sheet carrier density under the Schottky contact,

e is the unit electronic charge,

ε_s and d are the relative dielectric constant and the thickness of the InAlN barrier layer,

ε_0 is the permittivity of vacuum,

$e\phi_b$ is the Schottky barrier of the gate contact,

E_F is the Fermi level with respect to the GaN conduction-band-edge energy,

ΔE_c is the conduction band offset at the InAlN/GaN interface.

The InAlN/AlN/GaN Schottky diode can be modeled as two diodes back-to-back in series by introducing the effective conduction band offset $\Delta E_{c,eff}$, [17] as shown in the inset of Fig. 3a. In Eq. (1), $(e\phi_b + E_F - \Delta E_c)$ can be expressed in terms of Schottky barriers of the two diodes, $e\phi_{b1}$ and $e\phi_{b2}$, as

$$e\phi_b + E_F - \Delta E_c = e\phi_{b1} - e\phi_{b2} \quad (2)$$

Similar to Eq. (5) in Ref.[17], we can get

$$\phi_{b1} - \phi_{b2} = \frac{V_0}{n_1} \quad (3)$$

where V_0 is the flat-band voltage and n_1 is the ideality factor of diode 1. Substituting Eqs. (2) and (3) into Eq. (1), we obtain

$$\sigma/e = n_{2DEG} + \left(\frac{\varepsilon_s \varepsilon_0}{de} \right) \frac{V_0}{n_1} \quad (4)$$

n_{2DEG} can be calculated by *C–V* curve integration, and V_0 and n_1 can be obtained from forward current–voltage characteristics of the gate-source Schottky diode. The measured gate-source *C–V* curves and forward *I–V* curves for the InAlN/GaN HFETs are shown in Figs. 2, 3 and 4. Detailed calculations of n_{2DEG}, V_0 and n_1 are described in Ref.[17]. The barrier capacitance $\varepsilon_s \varepsilon_0/d$ is evaluated as the measured gate-source capacitance at zero bias.

Spontaneous polarization (P^{SP}) and piezoelectric polarization (P^{PE}) exist in the three layers of the InAlN/AlN/GaN heterostructure. Associated with a gradient of polarization in space is a polarization-induced charge density given by $\rho_P = -\nabla P$.[2] For the InAlN/AlN/GaN heterostructure, the polarization changes at an abrupt interface
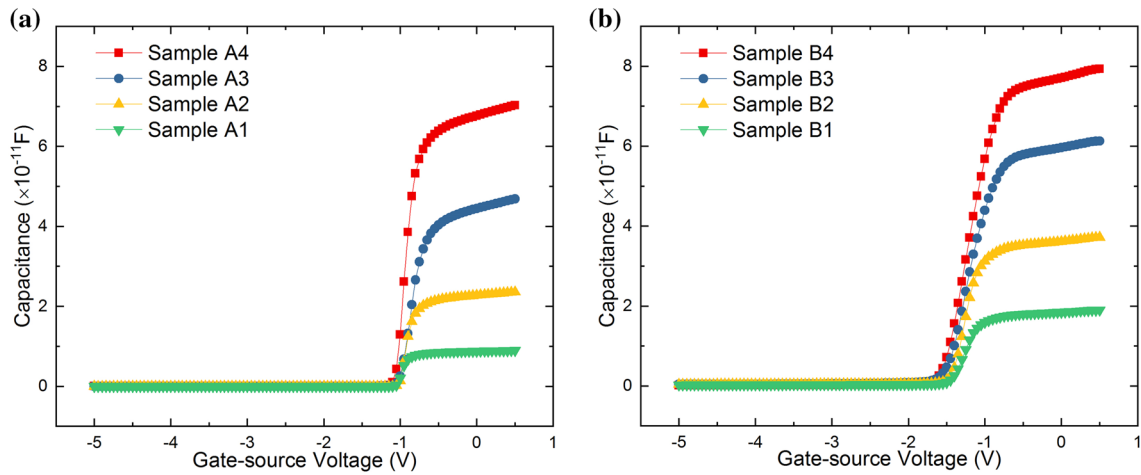
Fig. 2 Measured gate-source C–V curves for InAlN/GaN HFETs with normal-Ohmic contacts (**a**) and with side-Ohmic contacts (**b**)
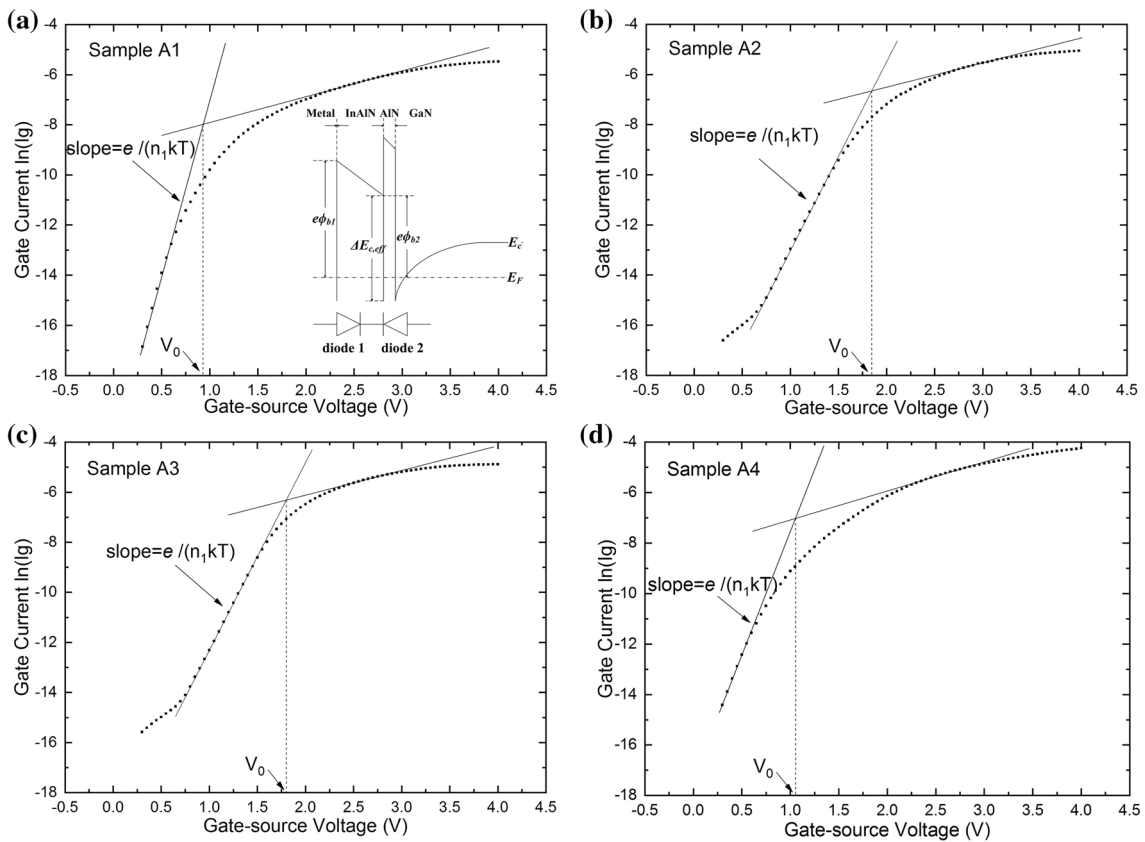

Fig. 3 Measured gate-source forward I–V curves for InAlN/GaN HFETs with normal-Ohmic contacts. Inset: the two-diode model and the conduction band diagram of the InAlN/AlN/GaN Schottky diode

of a top/bottom layer (InAlN/AlN or AlN/GaN), leading to the polarization sheet charge density at the InAlN/GaN interface of the InAlN/AlN/GaN heterostructure defined by [2]

$$\sigma = \left(P_{\text{GaN}} - P_{\text{AlN}}\right) + \left(P_{\text{AlN}} - P_{\text{InAlN}}\right) = P_{\text{GaN}} - P_{\text{InAlN}}$$
$$= P_{\text{GaN}}^{\text{SP}} - \left(P_{\text{InAlN}}^{\text{SP}} + P_{\text{InAlN}}^{\text{PE}}\right) \tag{5}$$

For the 2 μm-undoped GaN layer, the piezoelectric polarization can be neglected and only the spontaneous
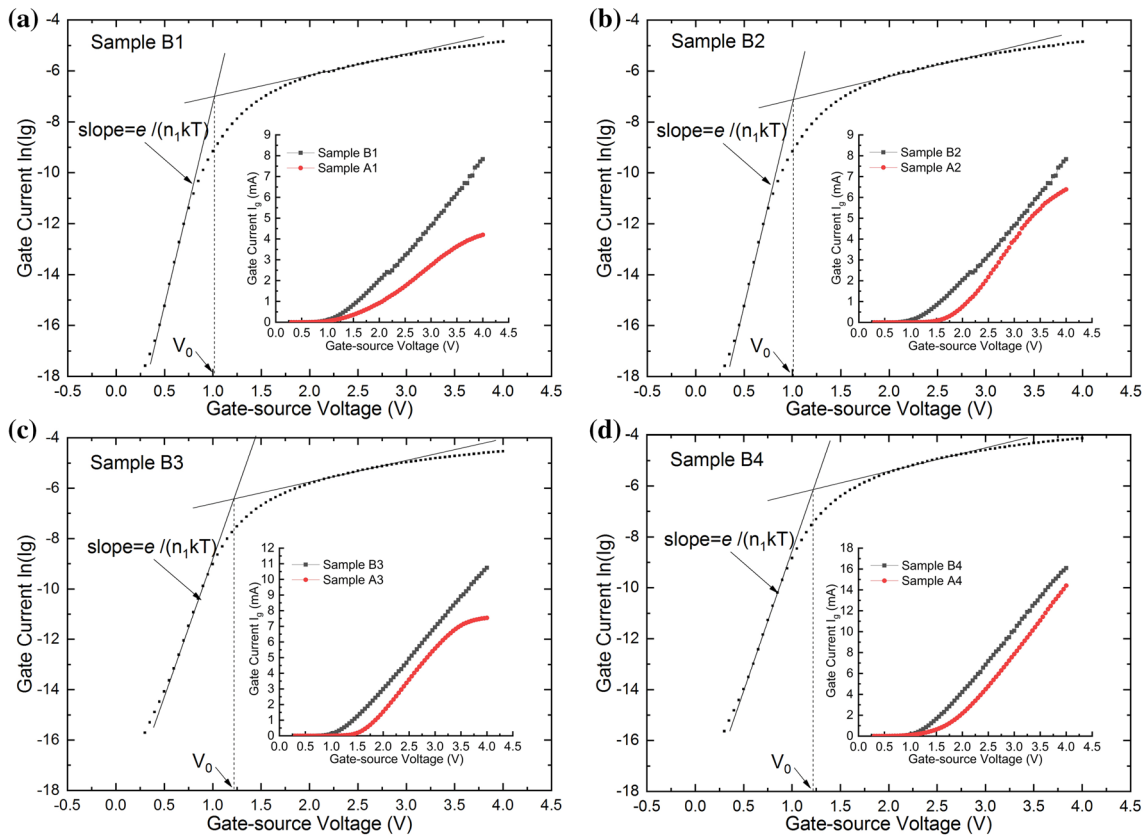
Fig. 4 Measured gate-source forward I–V curves for InAlN/GaN HFETs with side-Ohmic contacts. Insets: comparison of forward gate currents between samples with normal-Ohmic contacts and with side-Ohimc contacts

polarization is involved. A nonlinear polarization for nitride alloys of arbitrary composition is applied and the spontaneous polarization of InAlN and InGaN, in C/m², can be expressed as [15]

$$P^{sp}_{In_xAl_{1-x}N} = -0.042x - 0.090(1-x) + 0.071x(1-x) \quad (6a)$$

$$P^{sp}_{In_xGa_{1-x}N} = -0.042x - 0.034(1-x) + 0.038x(1-x) \quad (6b)$$

The piezoelectric polarization of the InAlN barrier layer can be calculated according to Eqs. (5), (6a), and (6b). With the piezoelectric polarization the in-plane compressive strain in the InAlN layer can be calculated as follows [15].

The piezoelectric polarization of the InAlN barrier layer can be expressed as

$$P^{PE}_{In_xAl_{1-x}N} = xP^{PE}_{InN}[\varepsilon(x)] + (1-x)P^{PE}_{AlN}[\varepsilon(x)] \quad (7)$$

The piezoelectric polarizations of the relevant binary compounds, in C/m², can be expressed as

$$P^{PE}_{AlN} = -1.808\varepsilon + 5.624\varepsilon^2, \quad (8a)$$

$$P^{PE}_{InN} = -1.373\varepsilon + 7.559\varepsilon^2, \quad (8b)$$

as a function of the in-plane strain

$$\varepsilon(x) = [a_{str} - a(x)]/a(x) \quad (9)$$

of the InAlN layer, with $a(x)$ and a_{str} corresponding to the lattice constants of the unstrained InAlN and of the strained InAlN, respectively.

Based on the above method, the in-plane strains in the InAlN barrier layers of InAlN/GaN HFETs of different gate lengths with normal-Ohmic contacts and with side-Ohmic contacts are determined and the results are shown in Fig. 5. For all samples, the InAlN barrier layers are compressively strained, which is consistent with the result in Ref.[11]. This indicates that the strain in the InAlN barrier layer should not be neglected especially when dealing with device instability problems. The reason for the compressive strain in the InAlN barrier layer of the lattice-matched In$_{0.17}$Al$_{0.83}$N/GaN HFET may be attributed to the Ohmic contact processing since it was pointed out that the Ohmic contact deposition and subsequent annealing could modify the strain state of the AlGaN layer in the AlGaN/GaN structure [18]. In Fig. 5,
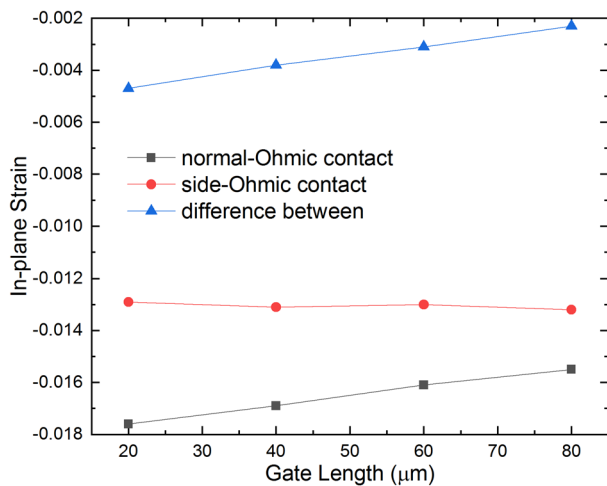
Fig. 5 The in-plane strains in InAlN barrier layers of InAlN/GaN HFETs with different Ohmic contacts

it also shows that there are obvious differences in the strain distributions between samples with different Ohmic contacts. The compressive strains in the InAlN barrier layers of samples with normal-Ohmic contacts are larger than samples with side-Ohmic contacts. Moreover, with the increasing gate length, the strain in the InAlN layer monotonously decreases for samples with normal-Ohmic contacts while it stays almost unchanged for samples with side-Ohmic contacts.

This Ohmic contact processing-dependent strain distribution can be explained by the difference in the laterally diffusing of Ohmic contact metal atoms into the InAlN barrier layer, which is not only similar to but also different from the explanations in AlGaN/GaN HFETs [12]. It has been demonstrated that for devices with side-Ohmic contacts there are no Ohmic contact metal atoms diffusing into the InAlN layer, while for devices with normal-Ohmic contacts a large number of Ohmic contact metal atoms diffuse into the InAlN layer and are located close to the Ohmic contacts within a much limited distance (1 µm or even shorter) [14, 19]. In this study, for samples with normal-Ohmic contacts, a large number of Ohmic contact metal atoms, including Ti, Al, Ni and Au, diffuse into the InAlN barrier layer after a rapid thermal annealing as illustrated in Ref [19]. by scanning electron microscope with energy-dispersive spectrometer (SEM–EDS). The reacted Al and Ti atoms can be introduced interstitially or by substituting N atoms and their radii are larger than that of N. Therefore the InAlN barrier layer between the source and drain contacts is squeezed, which is the same as mentioned in the AlGaN/GaN HFETs [12]. As a result, the compressive strain is enhanced as compared to samples with side-Ohmic contacts. The enhanced compressive strain, led by the inference of diffusing of Ohmic contact metal atoms into the InAlN barrier layer, in samples

with normal-Ohmic contacts weakens the total polarization of the InAlN layer, and consequently decreases the 2DEG sheet carrier density. That is why the forward gate current for samples with normal-Ohmic contacts is smaller than that of samples with side-Ohmic contacts as shown in the insets of Fig. 4.

The additional compressive strain introduced by the lateral diffusion of Ohmic contact metal atoms can be extracted to be the difference of strains between samples with normal-Ohmic contacts and with side-Ohmic contacts, as shown in Fig. 5. It decreases from the middle (corresponding to the sample with gate length of 20 µm) to the source/drain contact (corresponding to the sample with gate length of 80 µm), which is just opposite to the increasing trend in the AlGaN/GaN HFETs [12]. Consequently, there must be some other reasons, in addition to the squeezing effect on the InAlN barrier layer induced by the lateral diffusion of Ohmic contact metal atoms, for the monotonously decreasing strain distribution in the InAlN barrier layer of the InAlN/GaN HFET with normal-Ohmic contacts. An assumptive explanation is proposed here. It is noticed that the InAlN barrier layer thickness in this work is only 4 nm, much thinner than the AlGaN barrier layer (usually larger than 20 nm) in the AlGaN/GaN HFETs [12]. During the Ohmic contact annealing, a large number of Ohmic contact metal atoms diffuse into the InAlN barrier layer within a much limited volume close to the source/drain contact. As they accumulate, the compressive strain increases with the increasing squeezing effect on the InAlN barrier layer between the source and drain contacts. When it comes to the extent that the limited tiny volume cannot afford the accumulated Ohmic contact metal atoms any more, the crystal structure of the InAlN barrier layer is destroyed and the nearby component is relaxed. Of course a TEM cross-section and selected area electron diffraction patterns are needed to validate this hypothesis. The relaxation of the InAlN barrier layer decreases with the increasing distance apart from the source/drain contact. As a consequence, the additional compressive strain introduced by the lateral diffusion of Ohmic contact metal atoms is decreased from the middle to the source/drain contact and the monotonously decreasing strain distribution in the InAlN barrier layer is formed.

Experimental measurements, like photoluminescence, Raman spectroscopy or X-ray diffraction, are needed to directly demonstrate the differences in the strain distributions between the InAlN/GaN HFETs with normal-Ohmic contacts and with side-Ohmic contacts. But considering the InAlN barrier layer thickness of 4 nm, conducting those measurements and acquiring accurate results will be very difficult. It can be indirectly verified by the well-known polarization Coulomb field (PCF) scattering [14, 20, 21]. The PCF scattering originates from the non-uniform distribution of the polarization charge density at the

AlGaN(InAlN)/GaN interface. A larger non-uniform strain distribution of the barrier layer gives rise to a larger non-uniform distribution of the polarization charge density, indicating a stronger PCF scattering. In this study, the larger and non-uniformly distributed strain in the InAlN barrier layer indicates enhanced PCF scattering in samples with normal-Ohmic contacts in contrast to samples with side-Ohmic contacts. This can be verified by the fact that in InAlN/GaN HFETs with side-Ohmic contacts the PCF scattering is not the dominant scattering mechanism while in InAlN/GaN HFETs with normal-Ohmic contacts the PCF scattering dominates over the other scattering mechanisms [19]. Moreover, with the increasing gate length, the decreasing strain in the InAlN barrier layer gives rise to reduced PCF scattering in samples with normal-Ohmic contacts, which also coincides with the findings in Ref.[19].

4 Conclusion

In conclusion, the strain distributions in the InAlN barrier layers of $In_{0.17}Al_{0.83}N$/GaN HFETs are determined using gate-source capacitance–voltage (*C–V*) curves and forward current–voltage (*I–V*) curves. It is found that the compressive strain in the InAlN barrier layer is nearly uniformly distributed between source and drain contacts for devices with side-Ohmic contact processing while it is enhanced and monotonously decreased from the middle to the source/drain contacts for devices with normal-Ohmic contact processing. The monotonously decreasing strain distribution for devices with normal-Ohmic contact processing is attributed to the additional decreasing compressive strain from the middle to the source/drain contact introduced by the lateral diffusion of Ohmic contact metal atoms into the InAlN barrier layer.

References

1. O. Ambacher, J. Smart et al., J. Appl. Phys. **85**, 3222 (1999)
2. O. Ambacher, B. Foutz et al., J. Appl. Phys. **87**, 334 (2000)
3. A.F.M. Anwar, R.T. Webster, K.V. Smith, Appl. Phys. Lett. **88**, 203510 (2006)
4. J. Jungwoo and J. A. del Alamo, IEDM pp 1–4 (2006)
5. C. Rivera, E. Muñoz, Appl. Phys. Lett. **94**, 053501 (2009)
6. P. Makaram, J. Joh, J. A. d. Alamo, T. Palacios, C. V. Thompson, Appl. Phys. Lett. **96**, 233509 (2010)
7. G. Meneghesso, M. Meneghini et al., Microelectron. Eng. **109**, 257 (2013)
8. J. Kuzmik, IEEE Electron Device Lett. **22**, 510 (2001)
9. M. Neuburger, T. Zimmermann et al., Int. J. High Speed Electron. Syst. **14**, 785 (2004)
10. Y. Wang, Y. Lv et al., IEEE Electron Device Lett. **38**, 604 (2017)
11. Y. Zhou, Z. Lin et al., Semicond. Sci. Technol. **29**, 095011 (2014)
12. J. Zhao, Z. Lin et al., Superlattices. Microstruct. **79**, 21 (2015)
13. C. Luan, Z. Lin et al., Appl. Phys. Lett. **101**, 113501 (2012)
14. C. Luan, Z. Lin et al., J. Appl. Phys. **112**, 054513 (2012)
15. V. Fiorentini, F. Bernardini, O. Ambacher, Appl. Phys. Lett. **80**, 1204 (2002)
16. E.T. Yu, G.J. Sullivan et al., Appl. Phys. Lett. **71**, 2794 (1997)
17. Y. Lv, Z. Lin et al., Appl. Phys. Lett. **99**, 123504 (2011)
18. F. G.-P. Flores, C. Rivera, E. Munoz, Appl. Phys. Lett. **95**, 203504 (2009)
19. C. Luan, Z. Lin et al., Appl. Phys. A Mater. Sci. Process. **116**, 2065 (2014)
20. J. Zhao, Z. Lin, T.D. Corrigan, Z. Wang, Z. You, Z. Wang, Appl. Phys. Lett. **91**, 173507 (2007)
21. Y. Lv, Z. Lin et al., Appl. Phys. Lett. **98**, 123512 (2011)

Publisher's Note Springer Nature remains neutral with regard to jurisdictional claims in published maps and institutional affiliations.